Electronic Supplementary Information

Chemoprotective activity of mixed valence polyoxovanadates against diethylsulphate in *E.coli* cultures: insights from chemical speciation studies

Kahoana Postal[a], Daniela F. Maluf[a], Glaucio Valdameri[b], André Luis Rüdiger[a], David L. Hughes[c], Eduardo L. Sá[a], Ronny R. Ribeiro[a], Emanuel M. de Souza[b], Jaísa F. Soares[a], Giovana G. Nunes[a,*]

[a] *Departamento de Química, Universidade Federal do Paraná (UFPR), Curitiba-PR, Brazil. E-mail: nunesgg@ufpr.br*
[b] *Departamento de Bioquímica e Biologia Molecular, Universidade Federal do Paraná (UFPR), Curitiba-PR, Brazil.*
[c] *School of Chemistry, University of East Anglia, Norwich NR4 7TJ, UK.*

Table S1 Crystallographic parameters for complex **B**

Formula	$H_6PV_{14}O_{42}$, 3.5(NH_4), 0.5K, 12(H_2O)
Molar mass (g mol^{-1})	1721.06
Crystal system	Monoclinic
Space group	*C*2/*c*
a (Å)	11.7844(5)
b (Å)	24.2257(11)
c (Å)	16.3820(7)
β (°)	101.332(2)
V (Å^3)	4585.6(3)
Z	4
Density (mg m^{-3})	2.493
F(000)	3388
Absorption coefficient (mm^{-1})	2.93
Crystal size (mm)	0.024 x 0.16 x 0.23
θ range (°)	3.53 to 26.47
Reflections collected	61802
Unique data (R_{int})	4720 (0.048)
Observed data, ($I > 2\sigma_I$)	3953
Goodness of fit on F^2	1.041
R_1 ($I > 2\sigma_I$), wR_2 ($I > 2\sigma_I$)$^{(*)}$	0.025, 0.065
R_1, wR_2 (all data)	0.036, 0.069
Largest diff. peak and hole (e Å^{-3})	0.68 and -0.38

$^{(*)}$ $w = [\sigma^2(Fo^2)+(0.0387P)^2+9.61P]^{-1}$ where $P=(Fo^2+2Fc^2)/3$

Table S2 Selected bond lengths (Å) and angles (°) for the polyoxoanion in **B**, with estimated standard deviations in parentheses

Bond lengths (Å)

V(1)–O(1)	1.605(2)	V(1)–O(23)	2.364(2)	V(2)–O(20)	2.043(2)	V(8)-O(8)	1.608(2)
V(1)–O(21)	1.908(2)	V(2)–O(2)	1.606(2)	V(2)–O(23)	2.402(2)	V(8)-O(20)	1.820(2)
V(1)–O(15)	1.940(2)	V(2)–O(11)	1.728(2)	V(7)–O(7)	1.616(2)	V(8)-O(16)	1.910(2)
V(1)–O(13)	1.945(2)	V(2)–O(14)	1.948(2)	V(7)–O(19)	1.836(2)	P(1)–O(24)	1.549(2)
V(1)–O(11)	1.957(2)	V(2)–O(16)	1.955(2)	V(7)–O(18)	1.889(2)	P(1)–O(23)	1.536(2)

Angles (°)

O(1)-V(1)-O(21)	101.77(8)	O(19)-V(7)-O(19)#1	127.97(11)	V(2)-O(11)-V(1)	122.89(9)
O(1)-V(1)-O(15)	100.15(8)	O(7)-V(7)-O(18)	104.95(5)	V(4)#1-O(12)-V(3)	120.55(9)
O(21)-V(1)-O(15)	91.21(7)	O(19)-V(7)-O(18)	83.77(7)	V(4)-O(13)-V(1)	148.30(10)
O(1)-V(1)-O(13)	100.41(8)	O(19)#1-V(7)-O(18)	83.24(7)	V(3)#1-O(14)-V(2)	146.73(10)
O(21)-V(1)-O(13)	85.99(7)	O(18)-V(7)-O(18)#1	150.10(11)	V(6)-O(15)-V(1)	122.53(9)
O(15)-V(1)-O(13)	159.39(7)	O(8)-V(8)-O(20)	116.02(6)	V(8)-O(16)-V(2)	99.28(7)
O(1)-V(1)-O(11)	98.59(8)	O(20)#1-V(8)-O(20)	127.96(11)	V(8)-O(16)-V(6)	98.24(7)
O(21)-V(1)-O(11)	159.62(7)	O(8)-V(8)-O(16)	102.91(5)	V(2)-O(16)-V(6)	119.17(9)
O(15)-V(1)-O(11)	85.92(7)	O(20)#1-V(8)-O(16)	84.73(7)	V(5)-O(17)-V(3)	121.22(9)
O(13)-V(1)-O(11)	89.64(7)	O(20)-V(8)-O(16)	84.03(7)	V(7)-O(18)-V(5)#1	98.15(7)
O(1)-V(1)-O(23)	170.92(8)	O(16)#1-V(8)-O(16)	154.19(11)	V(7)-O(18)-V(4)	97.04(7)
O(21)-V(1)-O(23)	85.51(7)	V(2)-O(11)-V(1)	122.89(9)	V(5)#1-O(18)-V(4)	119.14(8)
O(15)-V(1)-O(23)	74.05(6)	V(4)#1-O(12)-V(3)	120.55(9)	V(7)-O(19)-V(4)	102.47(8)
O(13)-V(1)-O(23)	85.37(6)	V(4)-O(13)-V(1)	148.30(10)	V(7)-O(19)-V(5)	102.80(8)
O(11)-V(1)-O(23)	74.29(6)	V(3)#1-O(14)-V(2)	146.73(10)	V(4)-O(19)-V(5)	136.14(9)
O(2)-V(2)-O(11)	101.97(9)	V(6)-O(15)-V(1)	122.53(9)	V(8)-O(20)-V(6)#1	99.65(7)
O(2)-V(2)-O(14)	100.31(8)	V(8)-O(16)-V(2)	99.28(7)	V(8)-O(20)-V(2)	99.22(8)
O(11)-V(2)-O(14)	94.42(8)	V(8)-O(16)-V(6)	98.24(7)	V(6)#1-O(20)-V(2)	144.13(9)
O(2)-V(2)-O(16)	100.67(8)	O(19)#1-V(7)-O(18)	83.24(7)	V(5)-O(21)-V(1)	151.38(10)
O(11)-V(2)-O(16)	97.09(8)	O(18)-V(7)-O(18)#1	150.10(11)	V(3)-O(22)-V(6)	153.59(10)
O(14)-V(2)-O(16)	153.36(7)	O(8)-V(8)-O(20)	116.02(6)	O(23)-P(1)-O(23)#1	110.23(13)
O(2)-V(2)-O(20)	96.81(8)	O(20)#1-V(8)-O(20)	127.96(11)	O(23)-P(1)-O(24)	109.16(9)
O(11)-V(2)-O(20)	161.11(8)	O(8)-V(8)-O(16)	102.91(5)	O(23)#1-P(1)-O(24)	109.25(8)
O(14)-V(2)-O(20)	84.10(7)	O(20)#1-V(8)-O(16)	84.73(7)	O(24)-P(1)-O(24)#1	109.77(13)
O(16)-V(2)-O(20)	77.29(7)	O(20)-V(8)-O(16)	84.03(7)	P(1)-O(23)-V(1)	126.53(9)
O(7)-V(7)-O(19)	116.02(5)	O(16)#1-V(8)-O(16)	154.19(11)	P(1)-O(24)-V(4)	124.36(9)

Symmetry transformations used to generate equivalent atoms: #1 : 1-x, y, ½-z

Table S3 Hydrogen bonds, in Ångstroms and degrees, in crystal **B**.

O(12)-H(12)...O(13)#7	0.818(18)	2.05(2)	2.820(2)	156(3)
O(14)-H(14)...O(4)#8	0.832(19)	1.86(2)	2.683(2)	168(4)
O(17)-H(17)...O(31)#3	0.833(18)	1.821(19)	2.653(3)	176(4)
O(31)-H(311)...O(1)#9	0.855(18)	1.937(19)	2.772(3)	165(3)
O(31)-H(312)...O(17)	0.830(18)	2.26(2)	2.973(3)	144(3)
O(34)-H(341)...O(20)	0.850(19)	2.25(2)	3.061(3)	159(4)
O(34)-H(342)...O(2)#10	0.835(19)	2.47(4)	3.143(3)	138(5)
O(34)-H(342)...O(14)#10	0.835(19)	2.46(4)	3.066(3)	131(5)
O(35)-H(351)...O(16)	0.842(17)	1.918(18)	2.744(3)	167(3)
O(35)-H(352)...O(7)#6	0.840(18)	2.21(2)	2.961(2)	149(3)
N(41)-H(411)...O(34)#5	0.901(18)	2.20(2)	3.083(11)	167(6)
N(41)-H(412)...O(35)#5	0.898(18)	1.99(2)	2.879(15)	173(5)
N(41)-H(413)...O(33)#6	0.882(18)	2.34(3)	3.152(16)	152(5)
N(41)-H(414)...O(31)	0.876(18)	2.09(3)	2.943(13)	164(5)
N(42)-H(421)...O(34)#12	0.862(17)	2.025(18)	2.875(4)	168(4)
N(42)-H(422)...O(4)#1	0.886(17)	2.32(2)	3.148(3)	155(3)
N(42)-H(423)...O(35)#4	0.864(17)	2.030(17)	2.893(3)	177(4)
N(42)-H(424)...O(32)#13	0.864(17)	2.013(18)	2.873(4)	173(5)
O(43)-H(431)...O(15)#3	0.822(18)	1.96(2)	2.761(2)	166(4)
O(44)-H(441)...O(18)#1	0.868(19)	1.98(2)	2.821(3)	164(5)
O(44)-H(442)...O(11)#7	0.869(19)	2.01(2)	2.862(3)	165(4)

Symmetry transformations used to generate equivalent atoms:

#1 : -x+1,y,-z+½	#2 : x,-y+1,z-½	#3 : -x+½,-y+1½,-z+1
#4 : x+½,y+½,z	#5 : x,-y+1,z+½	#6 : x-½,y-½,z
#7 : x+½,-y+1½,z+½	#8 : -x+½,-y+1½,-z	#9 : -x,y,-z+½
#10 : -x+1,-y+1,-z	#11 : -x+½,y-½,-z+½	#12 : -x+1½,y+½,-z+½
#13 : x+1,y,z		

Table S4 Tentative assignments for the FTIR and Raman spectra registered for $K(NH_4)_5[H_6V_{14}O_{38}(PO_4)]\cdot 9H_2O$, complex **B** [1, 2]

Attributions	IR (cm^{-1})	Raman (cm^{-1})
ν(O–H)	3446	–
ν(N–H)	3357 – 3135	–
δ(O–H)	1628	–
ν(N–H)	1399	–
ν(P–O)	1053	–
ν(V=O)	936	990
ν_{as}(V–O–V)	726	691
ν(V–O)	588	–
ν_{s}(V–O–V)	–	523
δ(V–O–V)	–	405

Table S5 X-band EPR parameters for the mononuclear species detected at 77 K in LB solutions of products **A** and **B** with addition of DES

Components in solution[1]	***g*-Tensor**			**Hyperfine coupling constant (A) [10^{-4} cm^{-1}]**		
	g_y	g_x	g_z	A_y	A_x	A_z
A (aqueous medium)	1.9746	1.9777	1.9351	59.596	69.575	177.01
A + LB + DES	1.9746	1.9755	1.9410	55.763	62.960	169.60
B + LB + DES	1.9739	1.9752	1.9379	57.688	63.912	171.93

(a) Solution concentrations: **A** = 4.6 mmol L^{-1}, **B** = 5.0 mmol L^{-1} and DES = 6.0 mmol L^{-1}.

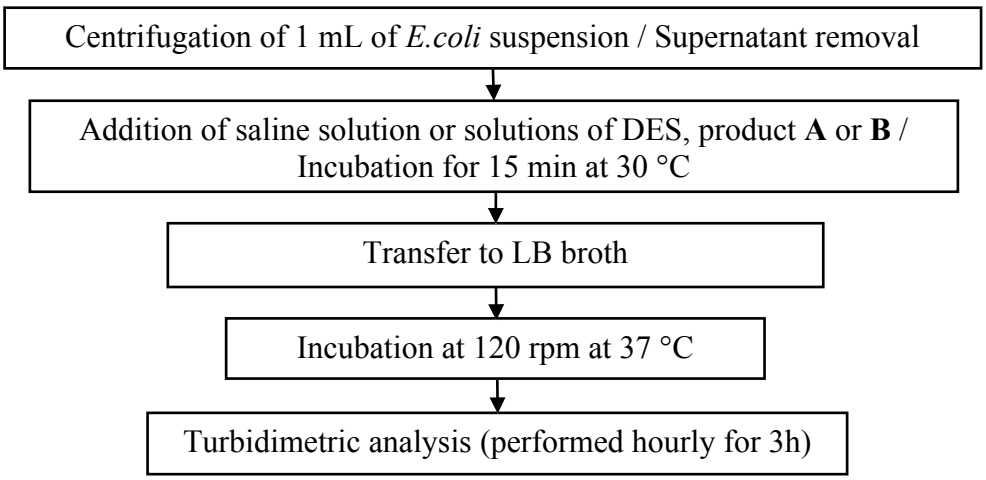

Scheme S1 Methodology adopted for analysis of the growth of *E. coli* cultures following addition of the alkylating agent, DES, and products **A** and **B** in different concentrations.

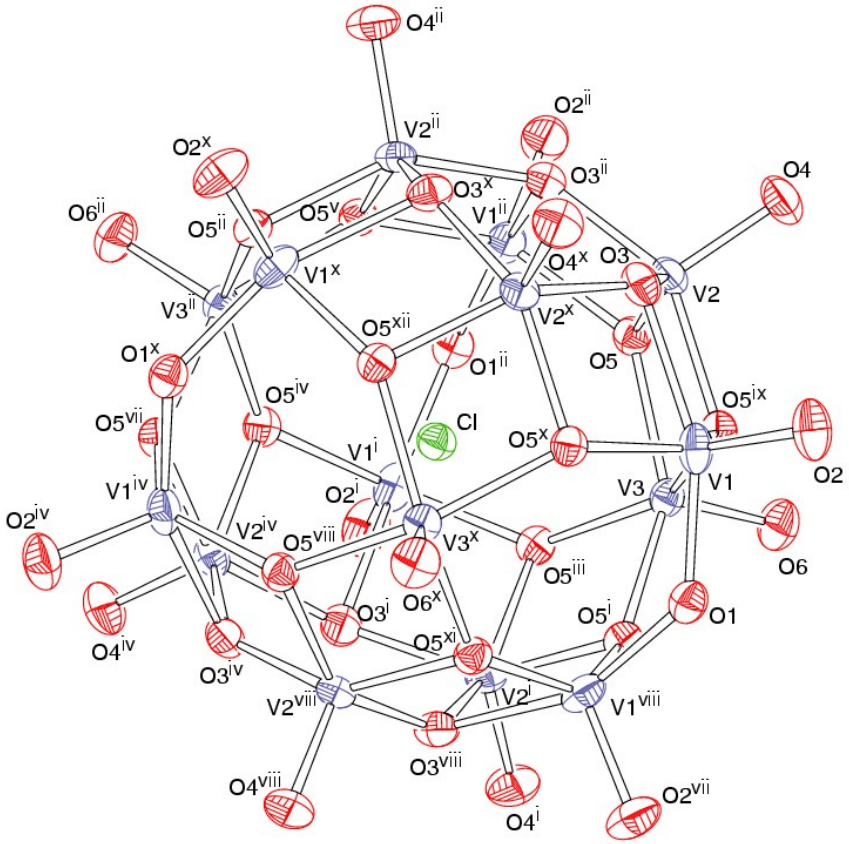

Fig. S1 ORTEP-3 representation of the polyanion in $(Me_4N)_6[V_{15}O_{36}(Cl)]$ (**A**).[3]

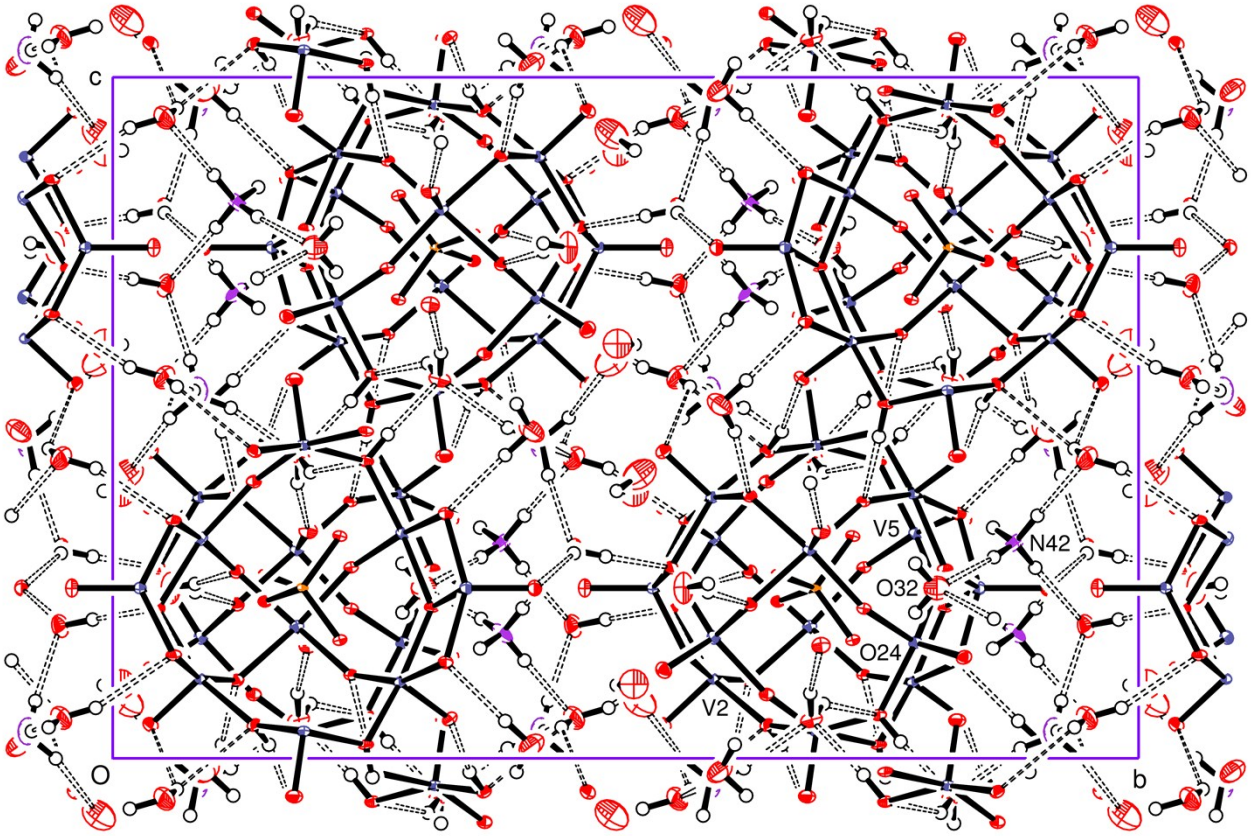

Fig. S2 Packing diagram for $K_{0.5}(NH_4)_{3.5}[H_6V_{14}O_{38}(PO_4)]\cdot 12H_2O$ (**B**) looking down the *a* axis and emphasizing the extensive hydrogen bond network in the crystal. The three crystallographically independent hydrogen atoms (H12, H14 and H17) are each involved in a hydrogen bond, with the acceptor atoms for two of these bonds lying in a neighbouring aggregate and the third in a well-defined water molecule, which also forms hydrogen bonds to two further polyoxoanions.

Several water molecules, a potassium ion (with partial-occupancy) and ammonium ions were identified in the crystal structure of **B** and many of the associated hydrogen atoms too. Most of the non-hydrogen atoms in this region were refined anisotropically. The hydrogen atoms were refined with O-H and N-H distance and angle constraints, with free refinement of isotropic thermal parameters, Figure S4 and Table S5.

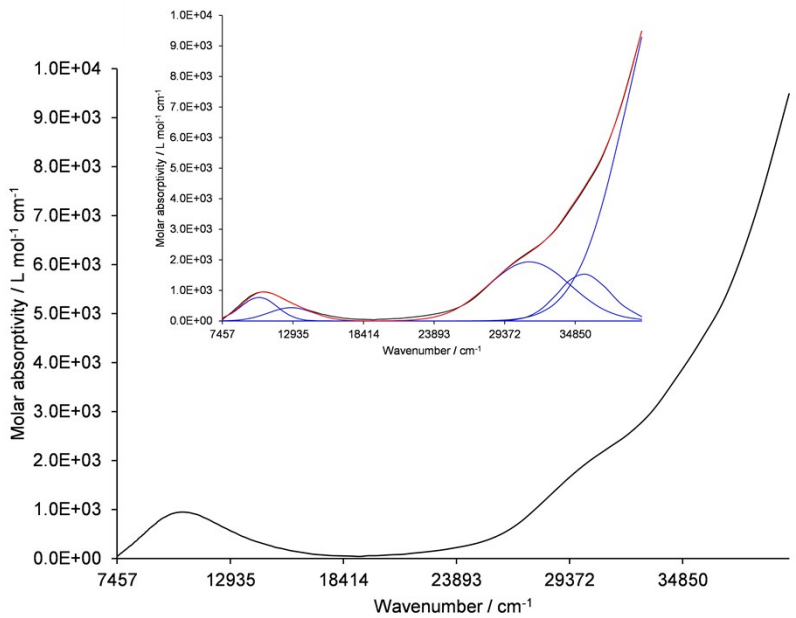

Fig. S3 UV/Vis/NIR spectrum of a 1.5 mmol L^{-1} aqueous solution of $(Me_4N)_6[V_{15}O_{36}(Cl)]$ (**A**). In the insert, the black line represents the experimental spectrum, while the bands obtained by deconvolution are shown in blue and the resulting, calculated spectrum is seen in red colour.

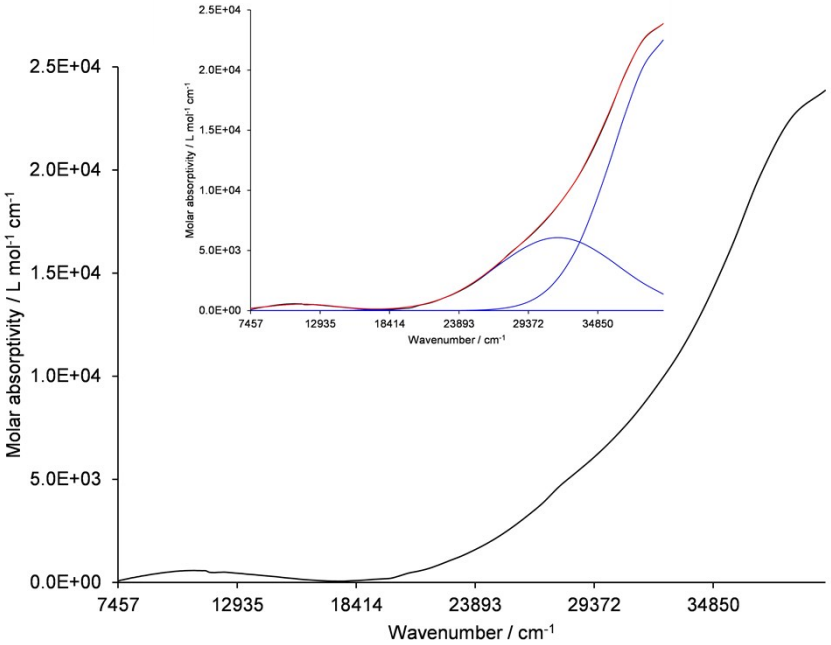

Fig. S4 UV/Vis/NIR spectrum of a 1.5 mmol L^{-1} aqueous solution of $K(NH_4)_4[H_6V_{14}O_{38}(PO_4)]\cdot 11H_2O$ (**B**). In the insert, the black line represents the experimental spectrum, while the bands obtained by deconvolution are shown in blue and the calculated spectrum is drawn in red. The more intense band that extends from 19000 cm^{-1} to the ultraviolet region is assigned to the LMCT p_π(O, oxo) $\rightarrow$ d_π(V) transition.[4]

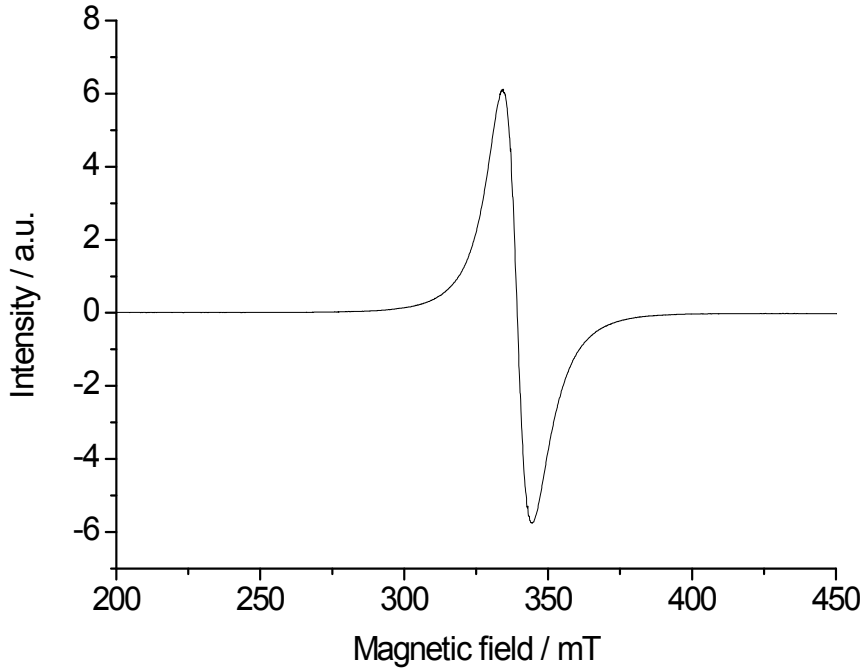

Fig. S5 X-band EPR spectrum recorded for **B** in the solid state at 77 K.

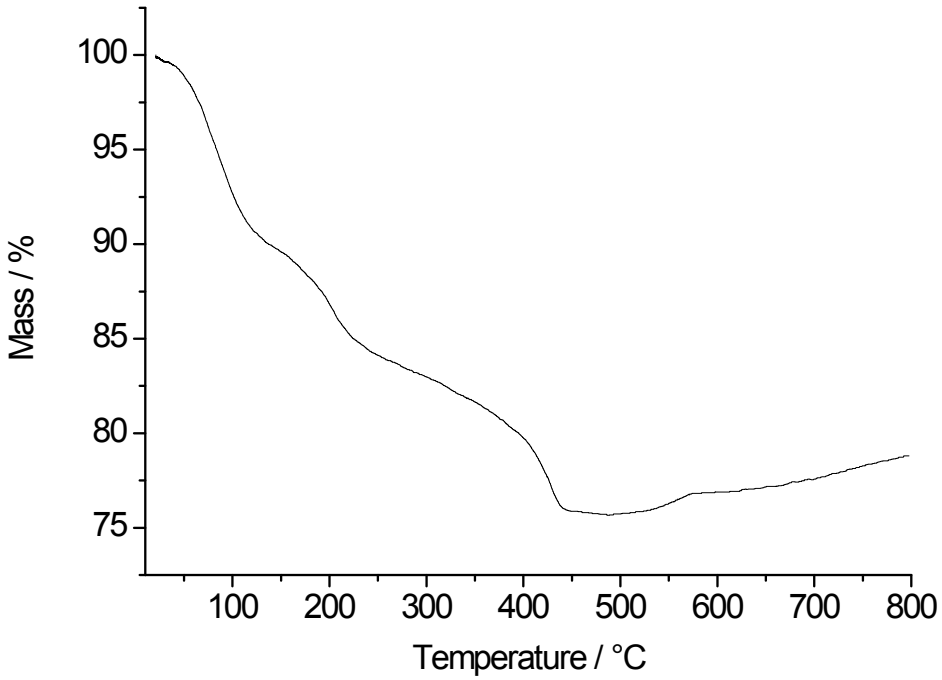

Fig. S6 Thermogravimetric analysis (TGA) profile obtained for product **B** in N_2 as carrier gas and temperature range of 20 to 800 °C.

The thermogravimetric analysis (TGA) of **B** revealed three main weight loss steps, from (i) 20 to 150 °C; (ii) 150 to 250 °C and finally from (iii) 250 to 450 °C. The first two are equivalent to the release of the 11 water molecules (crystallizing solvent) and four ammonium counter ions. In this temperature range, the total weight loss of 15.8% is consistent with the calculated value (15.6%).

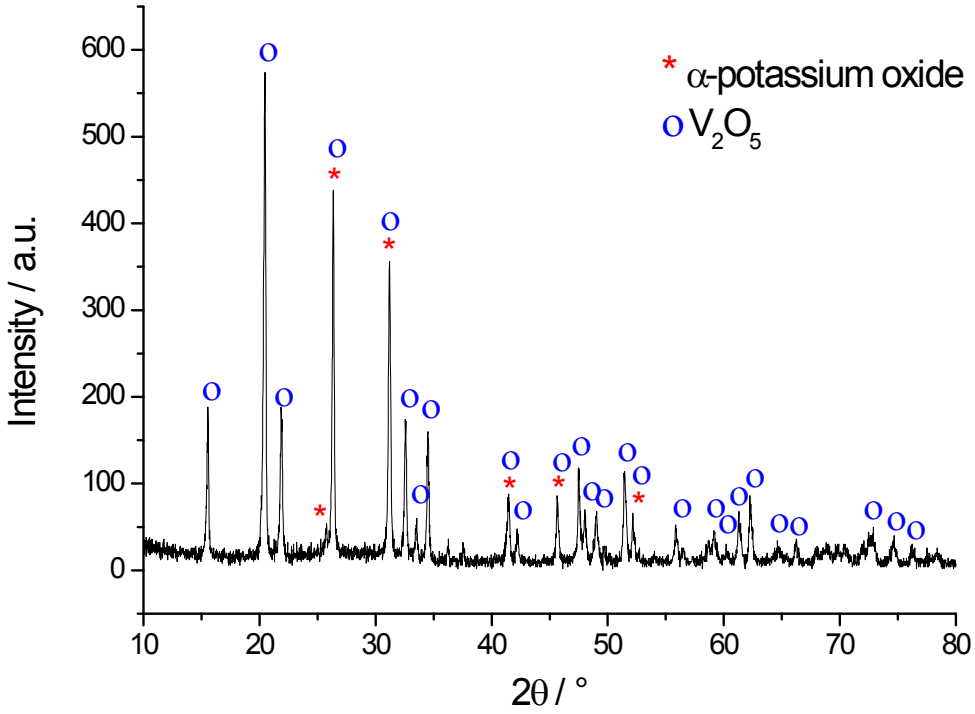

Fig. S7 Powder X-ray diffractometry of the oxide formed after thermal treatment of **B** at 550 °C. The observed peaks were attributed to V_2O_5 (JCPDS card number 41-1426) and α-potassium oxide (JCPDS card number 39-0697).

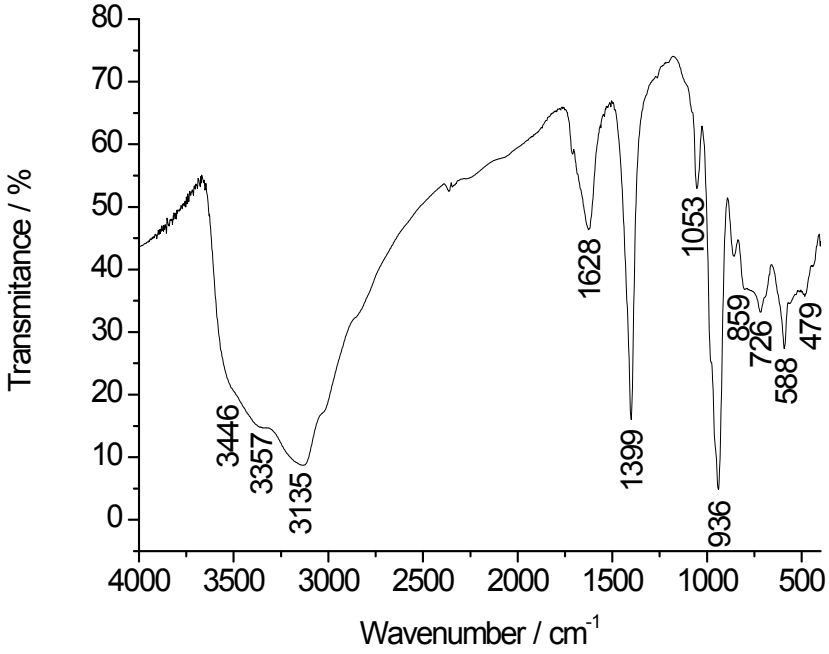

Fig. S8 FTIR spectrum recorded for product **B** (KBr pellet).

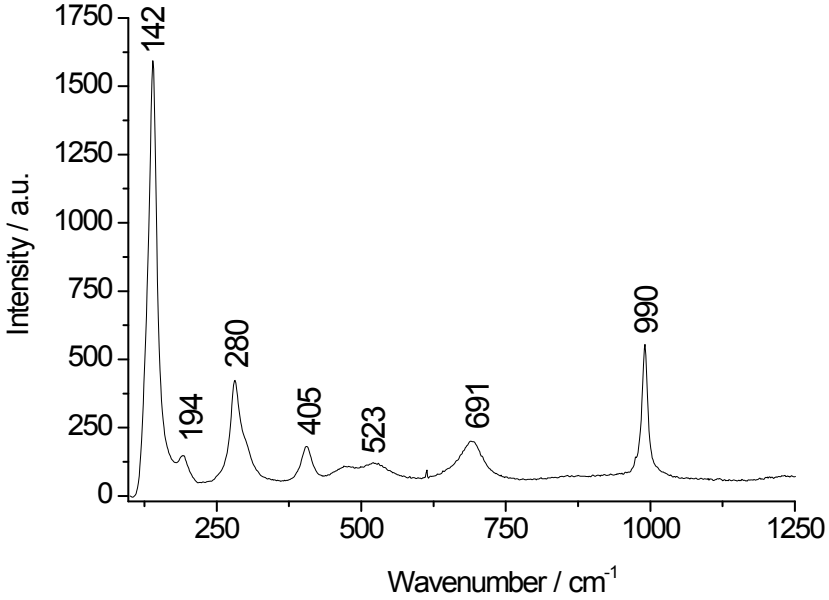

Fig. S9 Raman spectrum (He-Ne laser, 632.8 nm) recorded for **B**.

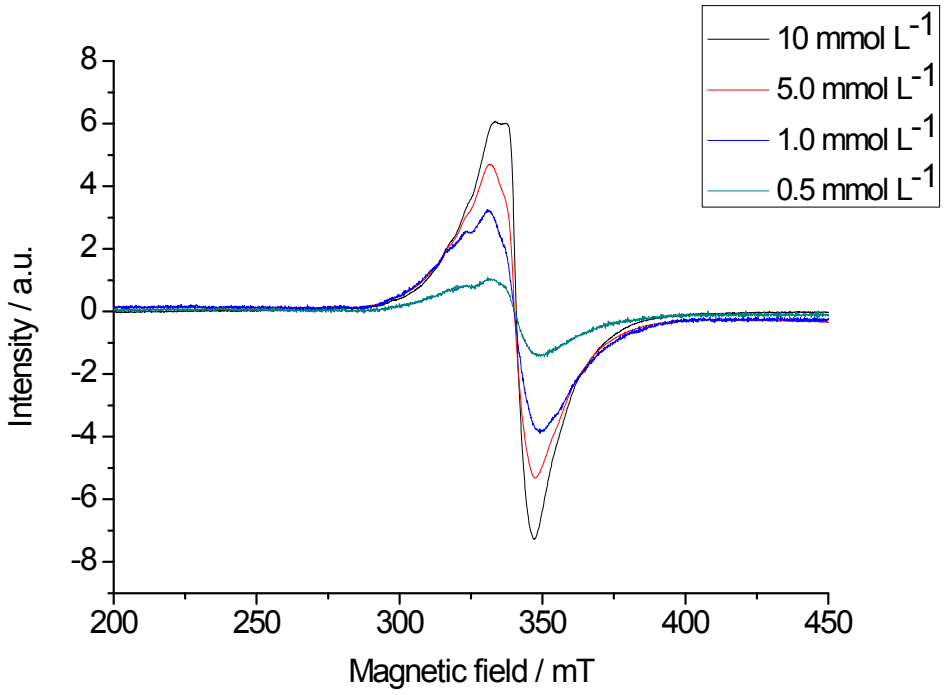

Fig. S10 X-band EPR spectrum recorded for aqueous solutions of **B** at 77 K in the concentration range of 0.5 to 10.0 mmol L^{-1}.

(a)

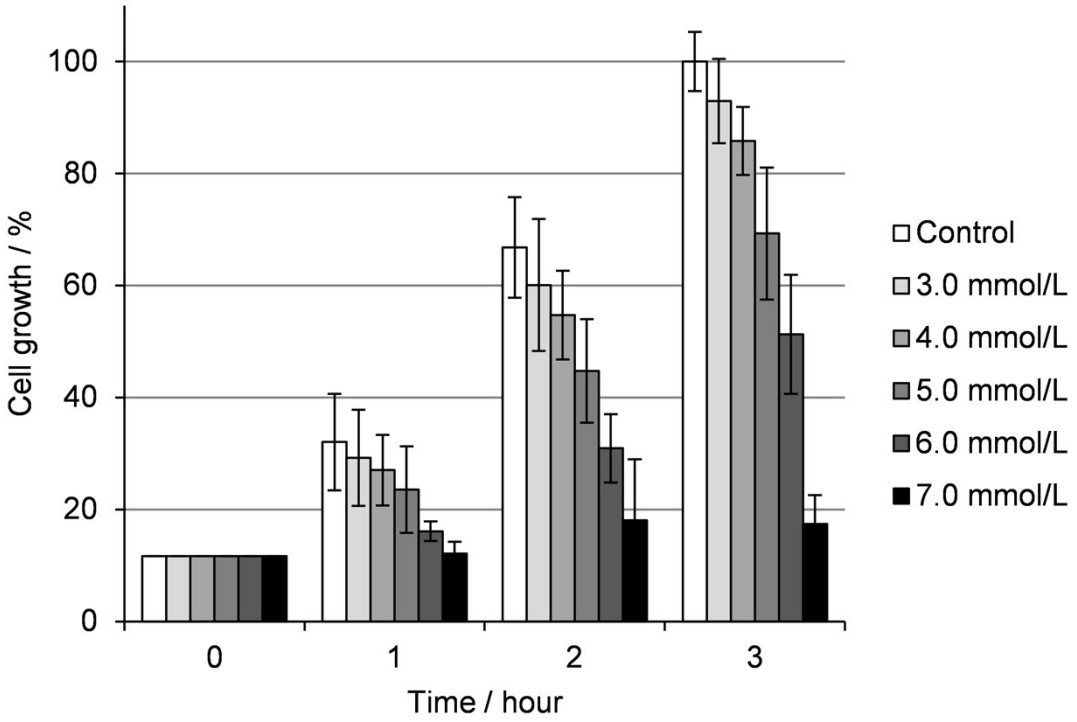

(b)

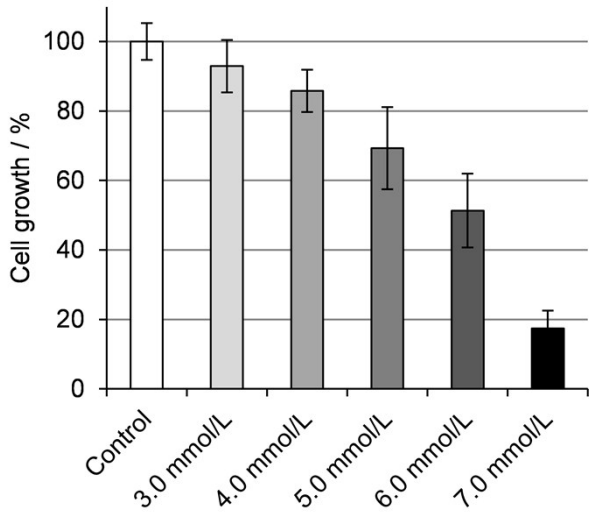

Fig. S11 (a) Growth of bacterial suspensions treated with increasing concentrations of the alkylating agent DES (3.0 to 7.0 mmol L^{-1}). From this experiment, a GI_{50} value of 5.8 mmol L^{-1} was determined. Concentrations are indicated by different colours as expressed in graphic *b*. In (a), cell growth values (in percentages) were plotted as a function of time, with average optical density values of 0.859±0.053 taken as 100% growth. (b) Growth of bacterial suspensions after incubation for 3 h with increasing concentrations of DES. Data are given as average values and standard deviations of triplicates.

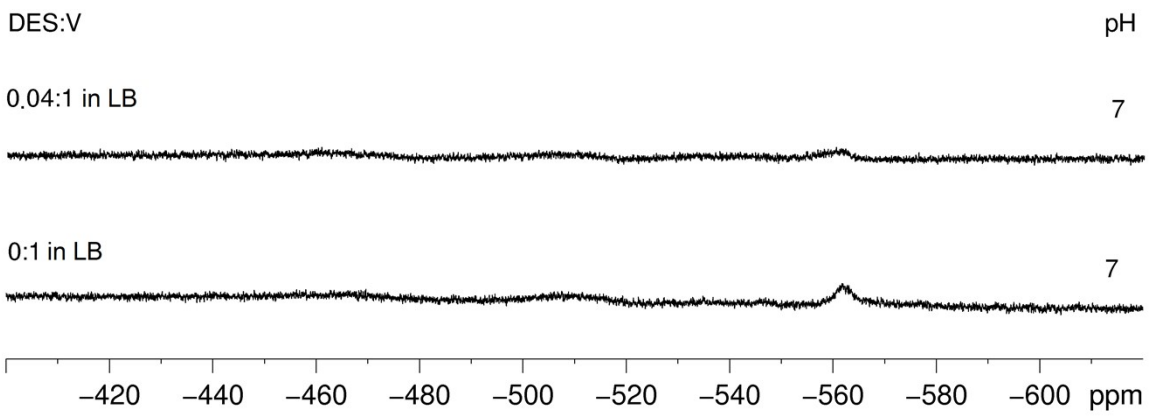

Fig. S12 ^{51}V NMR spectra of product **A** in LB at concentration of 10 mmol L^{-1} (bottom spectrum) and with the addition of 6.0 mmol L^{-1} of DES (top spectrum), in a DES:V proportion of 0.04:1.

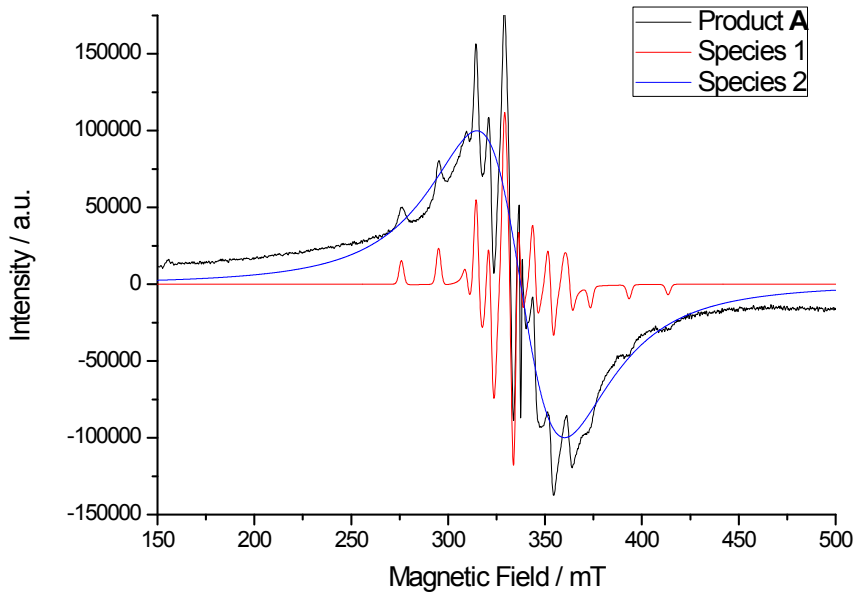

Fig. S13 X-band EPR spectra registered at 77K for product **A** in aqueous solution (4.6 mmol L^{-1}) and in the presence of the Cr^{3+} marker. Graphic shows experimental (black line) and simulated spectra, with the red and blue lines corresponding to the simulated mononuclear and polynuclear species respectively.

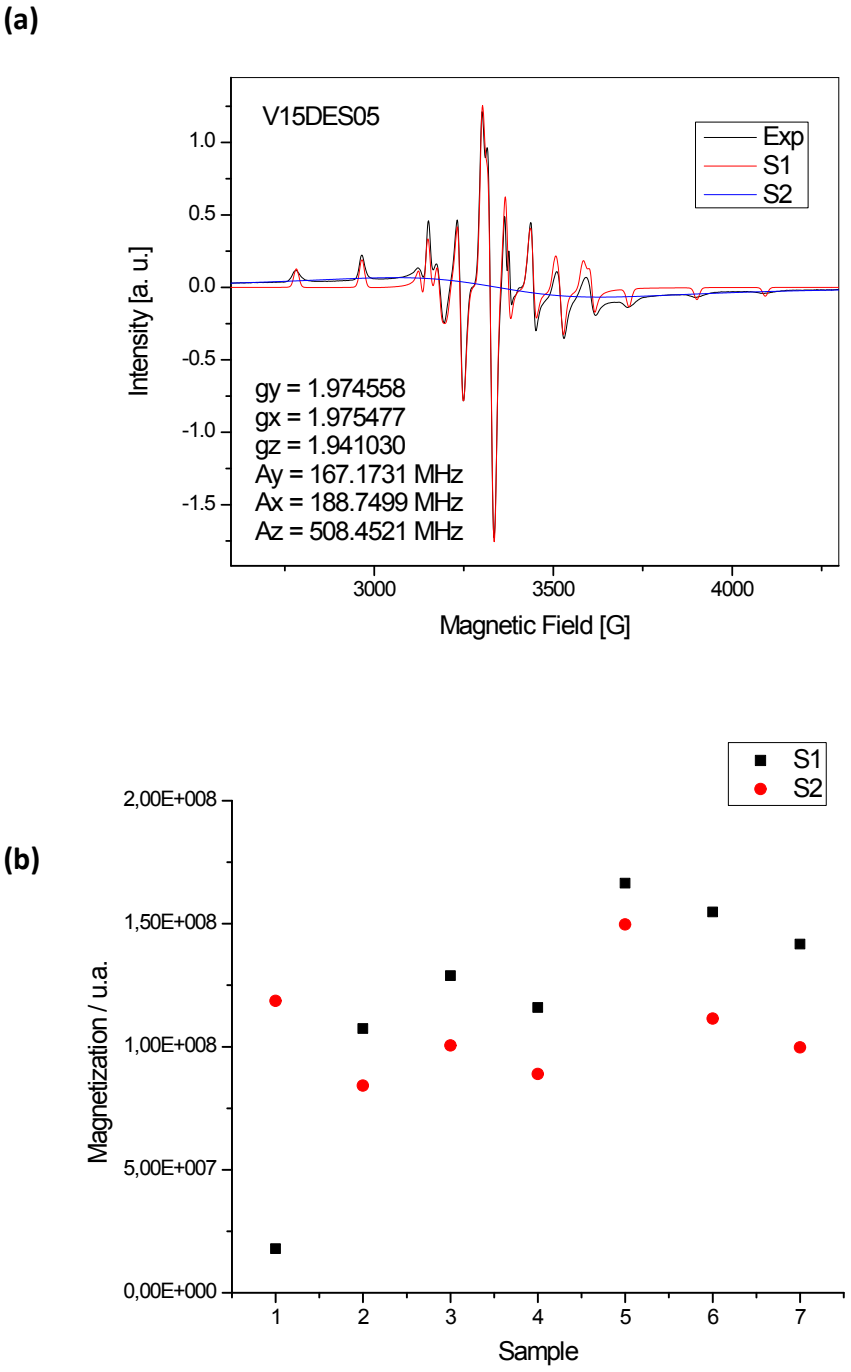

Fig. S14 X-band EPR data recorded at 77 K for **A** in the presence of DES. (a) Spectral simulations for the mononuclear (S1) and polynuclear (S2) species, with the calculated values of *g* and A for the mononuclear complex. The experimental spectrum is shown as a black line. (b) Relative contributions of the mononuclear (S1) and the polynuclear species (S2) to the total magnetization of the mixture. Samples listed in the x axis are: 1 – Aqueous solution of **A**, 4.6 mmol L^{-1}; 2 – Solution of **A** in LB, 4.6 mmol L^{-1}; samples 3 to 7 are solutions of **A** in LB, 4.6 mmol L^{-1}, with increasing concentrations of DES in the DES:V proportions of 0.05:1, 0.1:1, 0.5:1, 1:1 and 5:1, respectively.

(a)

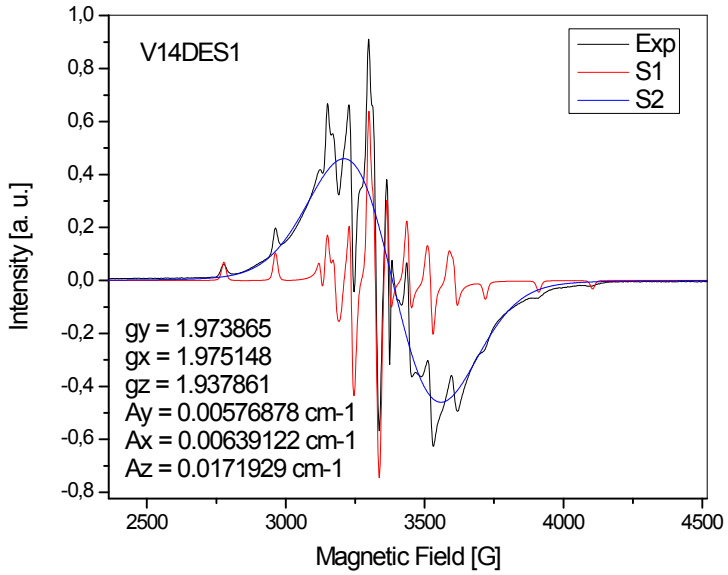

(b)

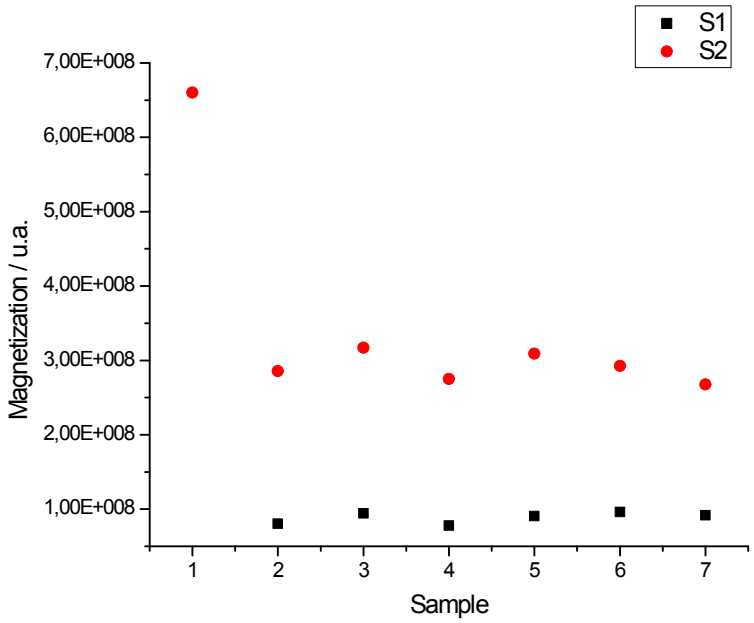

Fig. S15 X-band EPR data recorded at 77 K for **B** and DES. (a) Spectral simulations for the mononuclear (S1) and polynuclear (S2) species, with the calculated values of *g* and A for the mononuclear complex. The experimental spectrum is shown as a black line. (b) Relative contributions of the mononuclear (S1) and the polynuclear species (S2) to the total magnetization of the mixture. Samples listed in the x axis are: 1 – Aqueous solution of **B**, 5.0 mmol L^{-1}; 2 – Solution of **B** in LB, 5.0 mmol L^{-1}; samples 3 to 7 are solutions of **B** in LB, 5.0 mmol L^{-1}, with increasing concentrations of DES in the DES:V proportions of 0.05:1, 0.1:1, 0.5:1, 1:1 and 5:1, respectively.

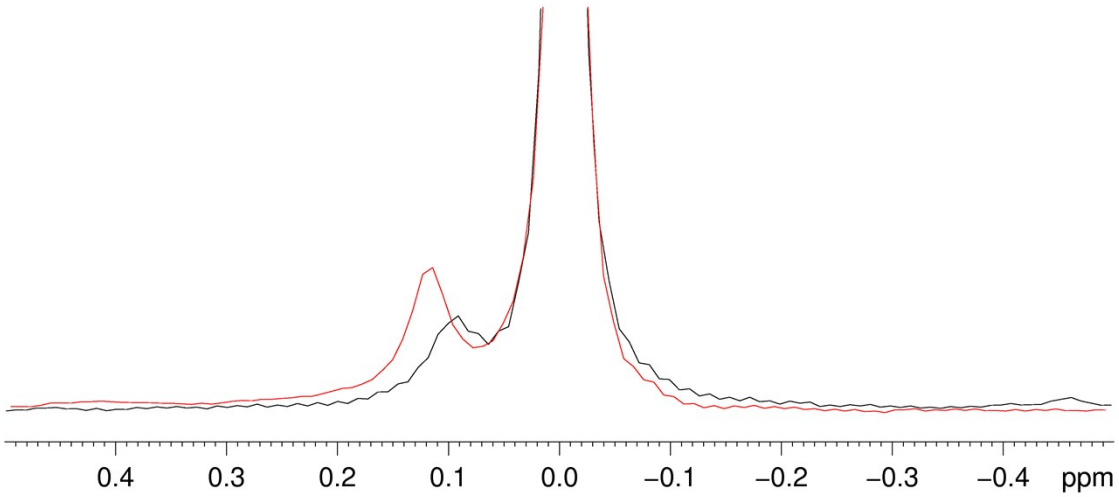

Fig. S16 ^{31}P NMR spectra (161.9 MHz) recorded for **B** with an external reference of H_3PO_4 (85%). Conditions were 5.0 mmol L^{-1} of **B** in LB medium (black line) and in LB medium with the addition of 6.0 mmol L^{-1} of DES (red line).

References

1. E. I. Voit, V. A. Davydov, A. A. Mashkovskii and A. V. Voit, *J. Struct. Chem.*, 2008, **49**, 13-20.
2. R. L. Frost, K. L. Erickson, M. L. Weier and O. Carmody, *Spectrochim. Acta A*, 2005, **61**, 829-834.
3. G. G. Nunes, A. C. Bonatto, C. G. de Albuquerque, A. Barison, R. R. Ribeiro, D. F. Back, A. V. C. Andrade, E. L. de Sá, F. d. O. Pedrosa, J. F. Soares and E. M. de Souza, *J. Inorg. Biochem.*, 2012, **108**, 36-46.
4. C. J. Ballhausen and H. B. Gray, *Inorg. Chem.*, 1962, **1**, 111-122.